

ZnO Nanocomposites in Dye Degradation



M. V. Manohar, Amogha G. Paladhi, Siji Jacob, and Sugumari Vallinayagam

Abstract Substances like dyes having substantial colouring capacity are used in textiles which releases the effluents into natural streams by evading waste water treatment. Pollution caused by such non-biodegradable dyes like making the water unfit for human activities, harming aquatic life, causing diseases in humans etc. has become the major concern. Advanced Oxidative Processes (AOPs) by photocatalysis are being employed to remove these dyes and bring a considerable reduction in the contamination. Various semiconductor nanoparticles are widely used for photocatalysed degradation of dyes, out of which ZnO nanoparticle is one of the effective catalysts for this purpose. ZnO is considered above all other metal oxides due to its stability, low cost, high photosensitivity and optical properties. ZnO is combined with metal, metal oxides etc. in order to overcome the recombination of generated charge carriers and increase its photocatalytic and sonocatalytic efficiency. ZnO is produced by several methods like hydrothermal synthesis, solvothermal synthesis, one step flaming process etc. Characterization and confirmation of the synthesized nanoparticles are carried out by techniques such as X-ray diffraction (XRD), UV–Visible analysis, Scanning Electron Microscopy (SEM), Transmission Electron Microscopy (TEM), Raman Spectroscopy, Brunauer-Emmer-Teller (BET) technique, Field Emission Scanning Electron Microscopy (FE-SEM), Energy Dispersal X-ray analysis (EDX), Fourier-Transform Infrared (FTIR) spectroscopy Analysis, Energy Dispersal X-Ray spectroscopy (EDS) etc. Photocatalytic and sonocatalytic dye degradation depends on pH, size of the ZnO nanocomposite and calcination process. In this review different methods of ZnO synthesis, nanocomposite synthesis of ZnO with metals, characterization of the ZnO nanoparticles and dye degradation processes have been discussed.

M. V. Manohar

JSS Medical College (Deemed to be University), Mysuru, Karnataka, India

A. G. Paladhi · S. Jacob

CHIRST (Deemed to be University), Bengaluru, Karnataka, India

S. Vallinayagam (✉)

Department of Biotechnology, Vel Tech Rangarajan Dr.Sagunthala R&D Institute of Science and Technology, Chennai 600062, India

e-mail: sugumariv@veltech.edu.in

Keywords ZnO nanocomposites · Dye degradation · Photocatalysis · Sonocatalysts · Nanoparticles · Dye decolourization · ZnO co-dope · Doping · Nanospheres · Dye · Calcination · Methylene blue · Methyl orange · Congo red · Azo Rhodamine B · Acid red B · Coomassie brilliant blue

1 Introduction

The water in natural bodies is contaminated due to the release of residual dyes from textile industries, dye producing and other industries. These residual dyes produced from textile industries are not easily biodegradable. Thus, contaminated water should be treated for the removal of these non-biodegradable dyes that are harmful to the biome [47, 50]. The dye affects the properties of water like colour, odour and physiochemical properties. There are different techniques involved in the treatment of dye-contaminated water. The principles for dye degradation are basically adsorption of dye by physical or chemical coagulations that can help the removal of textile dyes [47]. These are the advanced techniques used for the degradation of dyes which involves H_2O_2 , O_3 in the influence of irradiation that causes oxidative degradation of contaminants. The above process is termed as Advanced Oxidative Processes (AOPs). The technique of photocatalysis using semiconductor metal oxides is recently introduced AOPs that help in the easy removal of the dye by the principle of surface adhesion due to charge. ZnO (Zinc oxide), TiO_2 (Titanium dioxide), Fe_2O_3 (Hematite), WO_3 (Tungsten oxide) and ZnS (Zinc sulphate) are few light-sensitive semiconductors that use the principle of redox reactions due to their surface morphology. The morphology is due to the chemical combination possessing reliable characters of empty conduction bands and of filled valence bands [7]. As they are light-sensitive semiconductors, struck with irradiations of UV or natural light or other compatible source of light that can excite the electrons from valence band to conduction band forming an electron hole in the valence band. The electron and hole helps in the adhering of desired molecules (dye) to its surface due to the formed valency. The electron sharing assures the binding of dye molecules. Simultaneously in the process due to UV irradiation, ultrasound treatment splits the aqueous solution into hydroxyl ions [15] and superoxide radicals due to its lesser Electromotive Force [48]. ZnO having emV compared to other semiconductor photocatalysts is a very efficient nanoparticle that has significantly high molecular size compared to TiO_2 and has high catalytic capacity [7]. ZnO is found to be the most eligible nanoparticle among other semiconductor photocatalysts because of its property of harvesting the majority of the solar spectrum for its photocatalytic activity, also it is known to be very stable in the presence of sunlight [7].

These metal oxide semiconductor photocatalysts use UV light that is present in the spectrum of visible light where the percentage of UV light in visible light spectrum is very minimum, i.e. 5–7% [10]. To reduce or minimize the water cleavage due to the photocatalytic activity of ZnO under UV irradiation different transition metals are used as dopants. ZnO is usually doped with transition metals like Cu, W, Ni and N to

reduce the photoreactivity by producing more number of lone pairs of electrons. ZnO is known to be efficient for the degradation of dye in natural biomes because of its property to produce H_2O_2 more efficiently [6]. ZnO has more number of active sites that helps in the adhesion of the majority of the dye molecules due to its property of surface reactivity [33]. The aim is to study the preparation of ZnO, doping or co-doping, degradation of textile dyes, influence of different parameters that affects dye degradation and to review different studies and experiments based on the use of ZnO to degrade textile dyes.

2 Experimental Approach

2.1 Properties of ZnO Nanoparticles and Nanosphere

Among metal oxides, ZnO is an ideal photocatalyst. ZnO is stable, affordable and environment-friendly [22]. ZnO despite being photocatalyst also possesses the properties of sonocatalyst [58].

The assemblage and irregularly formed spatial arrangement in ZnO molecules are comparatively lower than that of adhered metal oxides. The above property of irregularly formed spatial arrangement and assemblage is a beneficial activity of ZnO as it provides increased active sites to adhere dye molecules more efficiently. The impurities like 2% Ni and 2% Al are doped with ZnO which causes the increase in the surface area of the catalyst which in turn facilitates the adsorption of dye adhering to the surface of doped ZnO catalyst. Hence, the doping of ZnO improvises the property of dye degradation [40].

2.1.1 Photocatalytic Property and Activity

The photocatalytic activity of ZnO can be elevated by doping ZnO with specific transition metals [21].

The Methyl Orange (MO) and Congo Red (CR) dyes are degraded using the photocatalytic activities of ZnO in visible-light spectra, where MO and CR are ideally used textile dyes which are also organic pollutants. The photocatalytic activity of ZnO is efficient in the presence of visible light for dye degradation. Ni is doped in a preferred quantity to elevate the efficiency of photocatalysis, if the doping of Ni exceeds the threshold quantity, it in turn causes the declination in the performance of ZnO resulting in the formation of oxygen vacancies on the grain and surface boundaries where the development of the nanoparticles is inhibited causing a stress field that further acts as the scattering centers to holes and electrons that avoids the recombination rate of hole–electron pairs. It was observed that these scattering centers enhance the photocatalytic activity [40, 50]. If Ni is doped in high quantities than threshold, it decreases the surface area for photocatalytic activity, because Ni

occupies majority of voids in the composition of ZnO nanoparticle, due to which the photon adsorption of ZnO declines [40]. The reactive species like Oxygen O_2 and hydroxide (OH^-) are significant in the process of photodegradation of dye [27].

2.1.2 Sonocatalytic Properties of ZnO

During sonolysis, water under high temperature and pressure, that occurs in short intervals generates free radicles, H^+ and OH^- having high oxidative potential. The free radicles thus produced react with each other to form Hydrogen Peroxide (H_2O_2) and Hydrogen (H_2) [17]. Hydrogen and Hydrogen Peroxide are produced during sonochemical reactions due to the ultra-sound that is used to process the reactions [2, 3]. These species are also called Sono-generated charge carriers that hinder the sonocatalytic efficiency [50]. The ZnO (doped or co-doped) must be aggregated with some other sonocatalytic semiconductors that can help the completion of effective degradation of dye which are organic pollutants [24]. Thus, semiconductors like TiO_2 , WO_3 , Fe_2O_3 or other efficient metal oxides can be co-doped for the preparation of nanocomposites [16].

2.2 Preparation

2.2.1 Synthesis of ZnO Nanospheres

The ZnO catalyst which is 99% pure is available in the market and can be used for photocatalysis or dye degradation without any further treatment/as such [7].

$ZnOCl_2 \cdot 8H_2O$, $ZnCl_2$ or $AlCl_3 \cdot 6H_2O$, $ZnCl_2$ or $AlCl_3 \cdot 6H_2O$ is used for the synthesis of ZnO nanoparticle using ultracentrifugation and hydrothermal synthesis method, where water or 1,2 ethanediol and aqueous NaOH of 5M is used to dissolve the above-mentioned complex molecule and calcinated at high temperature of 150 if dissolved in 1,2 ethanediol or calcinated at 90 °C if the complex is dissolved in water. The dissolved contents are centrifuged at 6000 rpm. The washing is done using H_2O and 2-propanol to eliminate the excess chloride ions, the process is otherwise known as peptization. Peptization helps in the prevention of unnecessary aggregation of nanounits which may result in declined results. Calcination using various temperatures is done for the nanounits that contain microaggregations that are separated and the disintegration of micro-aggregates is carried out in water or 2-propanol using ultrasound or sonocatalysis for multiple number of times [31].

The ZnO nanoparticles were prepared using hydrothermal synthesis procedure. ZnO was added to Teflon liner with a different mol% of WO_3 , a base (NaOH) and N-butylamine were blended gently and then kept sealed in a common autoclave for 12 h at high calcinating temperatures of 120 °C, then the compound was extracted and it was washed multiple times using distilled water and dried at room temperature [10].

2.2.2 Synthesis of Co-doped Nanospheres

The currently used dopes are the materials that possess multiple properties. Due to these multiple properties, dopes are used as composite materials that help to elevate the properties of individual compound containing nanospheres [5]. To exemplify, WO_3 -ZnO is more efficient than ZnO alone. The process of doping different species or compounds with individual nanospheres to enhance the efficiency without manipulating the original properties is called Co-doping.

CuO/ZnO nanocomposites are used where CuO is doped with ZnO nanocomposites for thermal decomposition under visible-light-driven photocatalytic dye degradation of textile dyes like Methylene Blue (MB) and Methyl Orange (MO) synthesized by Li et al. [27]. To assess the photocatalytic activity of ZnO/CuO nanocomposites, azo dye Rhodamine B (RhB), which is an organic pollutant discarded from textile industries, was experimentally used under water using the photodegradation process where Xe-lamp radiation is used [27]. To investigate photocatalytic dye degradation of Methyl Orange (MO) and Methylene Blue (MB) dyes by sunlight irradiations using carbothermal evaporation, CuO/ZnO nanocomposites were used by Kuriakose et al. [25].

Yu et al. used WO_3 /ZnO nanoparticles as photocatalyst by varying the concentration of WO_3 by precipitation grinding method where the above composite is desiccated at varied temperatures [17, 56]. The composite of WO_3 and ZnO was prepared by Adhikari et al. using known quantities of WO_3 and ZnO nanoparticles with varied ratios and determined that the ratio of ideal quantity of nanocuboid WO_3 and ZnO is 1:9 for the mixture to be efficient to photocatalytically decompose Methylene Blue (MB) and Methyl Orange (MO) accordingly [1]. Lam et al. prepared a very effective WO_3 -ZnO nanopowders using hydrothermal decomposition method and used the above nanoparticles for the degradation of 2,4-D (2,4-dichlorophenoxyacetic acid) using sunlight and revealed the use of WO_3 and calcined temperature resulted in effective photocatalytic activity [26]. WO_3 and ZnO nanopowders with varying WO_3 concentrations using a simple aqueous medium at lesser temperatures to determine the photocatalytic activities of WO_3 and ZnO nanoparticulations were used for the dye degradation. The dye degraded using the above method was Methyl Orange by Xie et al. [53].

Similarly, Ma et al. have formulated N/ZnO photocatalyst using thermal treatment protocols to elucidate the photocatalytic activity [20, 30]. The photocatalytic degradation of Methylene Blue was comparatively observed under visible range and UV light using N/ZnO nanoparticles by hydrothermal method. N/ZnO nanocomposites were composed and synthesized by Prabakaran et al. [37]. Sudrajat et al. used combustion reaction to prepare N/ZnO nanocomposites to determine the photocatalytic activity in Methylene Blue dye degradation [46].

Ni/ZnO nanoparticles were used as precursors to elevate the activity using co-gel or co-precipitation techniques and are compared to individual components to study dye-degradation [11, 27]. Chakrabarti et al. have compared the dye degradation capacity of ZnO nanoparticles to degrade organic dyes like Methylene Blue and Eosin Y, where 16 W lamp was used as the source of light and use of ZnO was accompanied by UV irradiation [7].

3 Characterization Techniques

3.1 X-Ray Diffraction (XRD)

It is one of the easy approaches for the determination of crystallite size of the powder samples. As the peak broadens, we can obtain a precise quantification of the particular sample [51]. Crystal structure of deposited samples was determined by using the X-ray diffraction patterns obtained with $\text{CuK}\alpha$ radiation ($\lambda = 1.5406 \text{ \AA}$) from a Bruker D 2 Phaser in the range of 20–50 °C by Y. M. Hunge et al. The XRD pattern of the $\text{WO}_3\text{-ZnO}$ nanocomposite could be indexed to the monoclinic and hexagonal crystal structures of WO_3 and ZnO, respectively. The crystallite size (D) was calculated using Debye–Scherrer's formula $D = 0.9 \lambda / \beta \cos \theta$ (where $\lambda = 1.5406 \text{ \AA}$ wavelength of the $\text{CuK}\alpha$ line, β is the Full Width at Half-Maximum (FWHM) for corresponding peak in radians and θ is Bragg's angle). Mean crystalline size of ultrasound-assisted WO_3 and $\text{WO}_3\text{-ZnO}$ nanocomposite was found to be 69 and 26 nm, respectively. Decreasing the crystallite size means increasing the specific surface area and hence increasing the sonocatalytic degradation rate [17].

Jun Wang et al. found the average size of the ZnO nanoparticles from the XRD patterns to be 33 nm according to the Scherrer's equation. The ZnO nanoparticles were used without any special treatments for the degradation process [52].

Karanpal Singh et al. characterized green synthesized ZnO nanoparticles using *Punica granatum* using PANalytical X-ray diffractometer at the range of angle from 0° to 100°. The XRD pattern revealed that the nanoparticles synthesized had a crystalline and wurtzite hexagonal structure which was confirmed comparing with JCPDS data sheet/ICDD no. 36–1451. The diameter was calculated according to the Debye–Scherrer's Equation and the average diameter was estimated as 20 nm [44].

3.2 UV–Visible Analysis

Synthesis of nanoparticles can also be confirmed by UV–Visible analysis. This technique works based on the principle of Beer–Lambert's law. The analyte concentration can be determined from the absorbance at a particular wavelength. The UV–visible absorption spectrum of green synthesized ZnO–Nanoparticles using *P. granatum* in the range of 200–800 nm in a quartz cuvette using Shimadzu UV Spectrophotometer. The absorbance peak was centered near 382 nm, indicating the reduction of zinc nitrate hexahydrate into ZnO nanoparticles [44].

Optical absorbance spectra of ZnO, Green AgNPs, ZnO–AgNPs–5 (5% green synthesized AgNPs) and ZnO–AgNPs–10 (10% green synthesized AgNPs) were analysed by using UV–vis (DRS)–NIR V-770 (JASCO, Japan spectrophotometer) in the wavelength range from 200 to 800 nm. At the end of the experimentation process, a black coloured powder which was Ag and the white coloured powder ZnO was obtained. As both the nanopowders were insoluble in MQ (Milli-Q)water, they

were subjected to sonication for 30 min to obtain a well-dispersed solution. Then the completely dispersed supernatant of the solution was taken into a quartz cuvette and exposed to UV–visible radiation. Here, maximum absorption of ZnONPs and AgNPs was observed at 410 and 390 nm which is in agreement with the reported values. With increasing the particle size, the absorption band shifts towards red. The inter-particle distance and the surrounding media also affect the absorption bands [19].

3.3 Scanning Electron Microscopy (SEM)

The surface morphology of green synthesized silver nanoparticles by Gangura leaves (AgNPs), ZnO powder, ZnO–AgNPs (5% green synthesized AgNPs) and ZnO–AgNPs (10% green synthesized AgNPs) were studied by Pranav Jadhav et al. using a Scanning Electron Microscope (Model JEOL-JSM-6360, Japan) which was operated at an acceleration voltage of 20 kV. The energy dispersive X-ray spectroscopy (EDAX) was carried out to check elements present in composites by using Oxford instruments INCA with SEM (S4800), Hitachi Japan. The nanoparticles were found to be spherical in shape with the diameter in the range of 1.1–1.5 μm . The shape, size distribution and morphology of the prepared ZnO–AgNPs–5% and ZnO–AgNPs–10% composites revealed that the major percentage of composites is in nanorods shape with the size lying in the range between 0.3 and 0.4 μm . The SEM images showed pebble-shaped ZnO nanopowder and rod-shaped AgNPs. The ZnO–AgNPs composites with different concentrations show an intermediate structure. The rod-shaped structures were found broken in the image which may have happened during grinding process [19].

Synthesized ZnO (N), Ag/ZnO (A) and Pt/ZnO (P) samples for 3 h (N3, A3 and P3) and 6 h (N6, A6 and P6) of reaction time, respectively, was subjected to analysis by L. Muñoz-Fernandez et al. using Scanning Electron Micrographs and EDS spectra. The micrograph of pure ZnO sample (N3) revealed the formation of quasi-aligned ZnO nanowires with a flat hexagonal top. Still an agglomerated structure was observed in hexagonal cross-sectional view of the top of the nanowires. The presence of Zinc and Oxygen peaks in the selected area of semi-quantitative analysis confirms the presence of pure zinc oxide according to XRD results. The micrograph of Ag/ZnO sample (A3) suggested that particles of noble metal mainly have a spherical morphology. Estimation of the real morphology was quite difficult due to the dense agglomeration and the heterogeneous sizes of ZnO.

Sample N3 and A3 presented quasi-aligned ZnO nanowires morphology. Micrograph of a Pt/ZnO sample (P3) also implied the nanowire morphology, which corresponds to ZnO.

EDS spectra displayed that chemical composition was based on pure Zinc, Oxygen and Platinum, being in good agreement with the XRD result. The micrographs of samples synthesized for 6 h were named N6, A6 and P6, respectively. These samples

exhibit similar morphology of nanowires that was obtained by the samples synthesized for 3 h, which again corresponded to ZnO particles. But in comparison, the growth of wires was rather uncontrolled, non-aligned and irregular when a longer reaction time was used. The differences in the morphology may be due to the kinetical growth control of certain crystal surfaces under different surfactants and electrostatic interaction between the positively charged facet of the ZnO crystal and charged chemical species. The nucleation of ZnO crystal and the preferred direction of crystal growth can be influenced this way by the surfactants. Cationic behaviors of surfactant like CTAB with similar molecular charge to the plane cause repulsion on the related plane boundary which can be the cause for change in the morphology [32].

3.4 *Transmission Electron Microscopy (TEM)*

This microscopic technique is used to describe the size and shape of nanoparticles. It uses a beam of electrons to focus the material and produce a highly magnified and clear image of it. TEM enables easy characterization of the image in its morphological features, compositions and crystallization information is also detailed. Jun Wang et al. found that the treated nanosized ZnO powders had a nanometer scale with the size around 30–45 nm, which was in accordance with the size calculated using Scherrer's equation (33 nm) [52].

Karanpal Singh et al. conducted the TEM analysis of green synthesized ZnO nanoparticles using *P. granatum*. The green synthesized ZnO-NPs were found to be polycrystalline with spherical structure and the size of the nanoparticles was in the range of 10–30 nm which correlated to the value obtained from the XRD data [44].

3.5 *Raman Spectroscopy*

The Fourier Transform Raman (FT-Raman) spectra of the prepared samples were collected in the spectral range of 100–1000 cm^{-1} using an FT-Raman spectrometer that applies Nd:YAG laser source with an excitation wavelength of 1064 nm. Raman spectroscopy is an inelastic light scattering method, where the energy transfers to and from the system under investigation are characteristic of electronic, optical, vibrational or even magnetic properties [9]. The structure and the symmetry of samples are studied using this method. The chief characteristic peaks for WO_3 were observed at 712.14 and 804.10 cm^{-1} . The peak centered at 436.38 cm^{-1} is the main characteristic peak of ZnO. The appearance of strong peak around 712.14, 804.10 and 436.38 cm^{-1} in a way suggested the formation of WO_3 -ZnO nanocomposites [17]. The Raman spectrum of layered WO_3/ZnO thin films were analysed by Y. M. Hunge et al. at room temperature in the range of 100 cm^{-1} . The Vibrational modes of the WO_3 sample, located at 272.60, 715.88 and 806.95 cm^{-1} , are due to the stretching and bending vibrations between O-W-O bonds of layered WO_3/ZnO thin films. The

peak at 132.13 cm^{-1} corresponds to the lattice vibrations in the WO_3 thin films. The two peaks were observed at 102.01 and 439.07 cm^{-1} in the layered WO_3/ZnO thin film, which are related to the Zn sub-lattice and the oxygen sub-lattice, respectively. The peak centered at 439.07 cm^{-1} confirmed that the synthesized samples have a hexagonal wurtzite phase [18].

3.6 Brunauer-Emmer-Teller (BET) Techniques

The surface area was analysed by nitrogen adsorption/desorption at 77 K using Gas Sorption System (Micro-metrics, Instruments, ASAP 2420). Inert gas adsorption technique is used to measure the specific surface area, pore size distribution and heats of adsorption. Surface area affects the dissolution rates, adsorption capacity and electron/ion current density, representing the free energy that is available for the bonding. Pore size also determines the performance of the material by affecting its diffusion rates, molecular sieving properties and surface area per unit volume [43]. So it is necessary to analyse, understand and confirm a particular material for better efficiency. Gas Sorption Analyzer records various pressures of gas in the sample cell due to adsorption and desorption. The instrument then calculates the amount (as STP volume) of gas adsorbed/desorbed. Surface area, pore size is calculated using computer software. Y. M. Hunge et al. measured nitrogen adsorption–desorption isotherms to examine the porous structure of WO_3 and $\text{WO}_3\text{-ZnO}$ nanocomposites by nitrogen adsorption/desorption at 77 K using a Gas Sorption System. BET surface area for $\text{WO}_3\text{-ZnO}$ nanocomposite was $57.1\text{ m}^2\text{ g}^{-1}$ which comparatively was higher than the pure WO_3 ($20.6\text{ m}^2\text{ g}^{-1}$). When observed, the results showed mesoporous structures of ZnO doped with WO_3 (ZnO/WO_3 nanospheres). With the increased surface area, WO_3/ZnO nanospheres are assured sonocatalytic nanoparticles that help in the degradation by providing more active sites on the surface due to the increased adsorption of dye molecules. This helps to elevate the effect of sonocatalysis [17].

3.7 Field Emission Scanning Electron Microscopy (FE-SEM)

Electron microscopy has been popular since 1944, when scientists Keith R. Porter and Albert Claude first used an electron microscope to observe the morphology and composition of cells. Imaging of the cells extends our scientific knowledge with respect to the morphology and the organization of organelles in cells. This technique also contributed to the modern improvements in molecular biology and medicine. Emergence of nanotechnology around 1959 has remodeled many of the tools and technologies required to view and interpret nanoenvironments [12].

As instrumentation and technology have evolved, scanning electron microscope is turning out to be a potent aid to analyse heterostructures and doping distributions on the nanometre scale. The introduction of Field-Emission Electron Guns coupled with the design of detector systems has made it possible to obtain high-resolution images over a wide range of acceleration voltages in the SEM. Scanning Electron imaging of any specimen may depend on microscopic parameters such as accelerating voltage, specimen tilt angle, beam current etc. It may also depend on the surface and bulk properties of the material [49]. FE-SEM is used to visualize and analyse every small topographic detail and thus used to determine the particle dimensions and morphology [44]. The morphological characterization of WO_3 and $\text{WO}_3\text{-ZnO}$ nanocomposite was studied by Y. M. Hunge et al. using a MIRA3 XMU TESCAN Field Emission Scanning Electron Microscope (FE-SEM). The samples showed uniform and compact surface morphology. The morphology of WO_3 structure exhibited an irregular distribution of nanoparticles, whereas the surface of $\text{WO}_3\text{-ZnO}$ nanocomposite showed round-shaped nanoparticles which efficiently increase the surface area for redox reaction usable for degradation of organic molecules. The effect of ultrasound causes empty spaces termed as cavities or voids that appear on the surface that effect the surface morphology and uniformity of the samples [17]. All the FE-SEM images of Green synthesized ZnO nanoparticles using *P. granatum* was found to be spherical shaped and the average particle diameter was 20 nm which corresponds to the XRD result [44].

3.8 Energy Dispersal X-Ray Analysis (EDX)

EDX is a technique that uses X-ray radiations to examine the composition of elements present in materials. It is a technique used to analyse the surface morphology of the sample where a beam of electron hits another electron present in the inner shell due to which it causes excitation. Due to the excitation of the electron present in the inner shell is ejected resulting in the formation of electron-hole or void in the composition of electrons in the outer shell of element. EDX systems are mainly used in electron microscopy instruments viz., SEM (Scanning electron Microscopy) or TEM (Transmission Electron Microscopy) instruments. The property of this electron excitation helps these instruments to produce the images of specimen that are microscopic. The data collected by EDX analysis contains a graphical representation where the peaks represent the respective spectra related to the corresponding elements. This helps us to know the actual composition of sample that is being analyse. The mapping of sub atomic particles like electrons in the sample helps in analyzing images that are obtained by SEM and TEM. The element analysis or chemical characterization of green synthesized ZnO nanoparticles was done using EDX by Karanpal Singh et al. and the EDX spectrum showed the presence of ZnO and O^- ions in ZnO nanoparticles synthesized using *P. granatum*. The elemental analysis of the ZnO powder indicated that 76% of Zinc and 15% of Oxygen were present which inferred good purity and very little impurities [44].

3.9 Fourier-Transform Infrared (FTIR) Analysis

To obtain the analysis of interfaces to analyse the adsorption of functional groups on the surface of nanoparticles, FTIR analysis is used. The molecular data analysed with the help of FTIR helps the investigator to interpret the conformational and structural changes of the self-aggregated functional groups that are adhered on the surface of nanoparticles. By analyzing the vibrations and rotations of molecules that are influenced by IR (Infra-Red radiation), a particular wavelength to which FTIR analyses spatial arrangement. There are few advantages that attribute for a better assessment in this technique viz., high accuracy, high stability, high signal-to-noise ratio and high energy. Karanpal Singh et al. carried out FTIR spectroscopy to confirm the formation of Zn–O bond and to identify the phytoconstituents of *P. granatum* that are capped on ZnO–NPs surface. Using a Bruker Alpha FTIR spectrometer, spectrum of green synthesized ZnO–NPs was analysed. The spectral peaks 3610 and 3822 cm^{-1} are due to O–H stretching. The peak around 2354 cm^{-1} is due to C–H stretch. The peak around 1512 cm^{-1} is due to the C=O stretching. The peak at 1683 cm^{-1} corresponds to ZnO bending deformation vibrations. The strong vibrational bands at 610 cm^{-1} are assigned to the stretching modes for the formation of ZnO nanoparticles. Thereby in this study it is clear that the ZnO–NPs were devoid of being aggregated by the phytoconstituents and also confirms the stability of the surface of nanoparticles during the synthesis [44].

3.9.1 Energy Dispersal X-Ray Spectroscopy (EDS)

EDS (Energy Dispersal X-Ray Spectroscopy) is a prescribed technique used for the identification of materials. A primary beam is used to obtain characteristic X-rays by placing the EDS systems on SEM (Scanning Electron Microscope). The analysis of the sample is done using the X-rays obtained, which are very particular to the samples. The intensity of the primary beam and the material of the samples are two factors on which the spatial arrangement or resolution of EDS depends [13]. Deducing the structure of atoms, identification and the site that are void can be occupied to know the magnetic properties [38]. The chemical composition of WO_3 –ZnO nanocomposite was examined using Energy Dispersive X-ray Spectroscopy (EDS) system attached to an FE-SEM (M MIRA3 XMU Tescon Orsay Holding) and the EDS pattern studies of WO_3 –ZnO nanocomposite prepared by sonochemical route ruminates the presence of W, Zn and O elements. The atomic percentage of the W and the Zn elements in the WO_3 –ZnO nanocomposite were found to be 32.56% and 22.18%, respectively. Thus, EDS results in addition to Raman and XRD results confirm the formation of WO_3 –ZnO nanocomposites [17].

4 Methods of Dye Degradation

4.1 Photocatalytic Degradation

Karanpal Singh et al. carried out photocatalytic degradation of Coomassie Brilliant Blue R-250 dye using Green synthesis of Zinc Oxide nanoparticles (ZnO-NPs) using *P. granatum* leaf extract. The process was carried out in an aqueous solution under sunlight. The powdered dye was dissolved in deionized water to which ZnO nanoparticles were added and sonicated. The mixture was stirred continuously for 30 min in the presence of sunlight. Four millilitres of the solution was centrifuged to pellet down at regular time intervals to check the absorbance at 600 nm which was the optimum absorbance peak of the dye. It was clearly observed that with time the intensity of blue colour of the dye solution decreased gradually and became light at last. ZnO-NPs could degrade the pollutant drastically in 3 h [44].

Pranav Jadhav et al. investigated the degradation efficiency of ZnO nanomaterials doped with Green synthesized silver (Ag) nanoparticles using Gongura leaves on Methylene Blue by photocatalytic degradation process. To 500 mL of distilled water, 5 mg of MB dye was added slowly for the preparation of dye. The dye preparation was completely carried out in dark. The prepared dye solution and the synthesized nanomaterials such as ZnO, ZnO-AgNPs-5 (5% green synthesized AgNPs using Gongura leaves) and ZnO-AgNPs-10 (10% green synthesized AgNPs using Gongura leaves) were added in separate beakers as a catalyst along with pre-prepared dye sample in the proportion of 1:1 (i.e. 50 mL of dye and 50 mL of catalyst) ratio. One beaker containing only dye solution was maintained as control. The beakers containing catalysts were stirred on magnetic stirrer for 30 min so that the dispersion is uniform. The photocatalytic treatment was carried out in the presence of sunlight at the ambient temperature in between 25 and 30 °C. The 1 mg/mL of concentration of ZnO nanoparticle was used for dye solution. The photocatalytic degradation progress was monitored at different intervals. The percentage of degradation was calculated by Degradation percentage (%) = $(C_0 - C_e)/C_0 \times 100$, where C_0 and C_e are the dye initial concentration and dye concentration after the photocatalytic treatment, respectively. The dye solution before the addition of the catalyst was exposed to sunlight and the spectrophotometric analysis of the sample after 15 min interval revealed that 37.76% dye was degraded under the sunlight which took about 120 min. The absorption spectra were recorded in the wavelength range between 400 and 800 nm. The absorption peak of Methylene Blue dye was found to be 664 and 614 nm in the visible region. Peaks are found to be decreased with an increase in time intervals due to redox reactions. Once ZnO was added to the Methylene Blue as catalyst, 91.67% degradation was observed after 120 min. Composites of ZnO-AgNPs-5 and ZnO-AgNPs-10 were added to the Methylene Blue, showing 99.21% and 97.71% dye degradation within 75 min, respectively. Composites of ZnO-AgNPs-5% proportion showed the better results of all as mentioned above [19].

4.2 Sonocatalytic Degradation

The sonocatalytic degradation is a novel technology for treating wastewater. It is an advantageous method over photocatalytic degradation as it uses low-power ultrasonic irradiation as the excitation energy for the degradation to take place. Ultraviolet light costs a lot of energy to induce semiconductor catalyst and also the photocatalytic degradation is not feasible for low transparent organic wastewater [52].

Y. M. Hunge et al. in his work used sonocatalytic procedure for Brilliant Blue dye degradation. The sonocatalytic degradation was executed using an ultrasonic bath under 200 W output power and 40 kHz frequency in the presence of prepared $\text{WO}_3\text{-ZnO}$ nanocomposite. As less number of OH^- radicals were formed in the sonolysis degradation alone, $\text{WO}_3\text{-ZnO}$ nanocomposite prepared with ultrasonic bath was an effective support for enhancing the sonocatalytic degradation efficiency. All reactions were performed under normal temperature and pressure. In this method, the prepared samples (0.2 g) and oxidants were added into 100 ml of 0.5 mM Brilliant Blue solution and then it is filled into the reaction container (150 ml). The reaction mixture was stirred for 15 min to attain adsorption–desorption equilibrium. A 4-ml sample was pipetted from the reaction mixture and centrifuged for 10 min. Once the catalyst was settled down the absorbance of Brilliant Blue solution was measured using an ultraviolet–visible (UV–vis) spectrophotometer [17].

The phenomenon of luminescence caused due to sonocatalysis is because of acoustic cavitation that results in the formation of beam of wavelength 420 nm. These beams of short wavelength generated has sonoluminescence induce WO_3/ZnO nanoparticles to produce lone pair of electrons that causes electron holes. Thus, generated electrons are excited from the conduction band of ZnO to the conduction band of WO_3 and the holes are shifted from valence bands of WO_3 to valence band of ZnO. This exchange of holes and electrons must be avoided to improve the dye degradation efficiency of nanoparticles (WO_3/ZnO nanocatalyst). The formation of holes has its negative impact on the adsorption of dye on the surface of photocatalytic nanospheres by degrading the nanospheres in the aqueous solution by producing OH from H_2O molecules. The presence of degraded nanoparticles in the solution causes the activation of sites that are responsible for producing acoustic cavitation. The bubbles produced due to cavitation settle on the surface, which causes the formation of more cavitation bubbles [17].

During the course of sonocatalytic degradation, UV–Visible absorption spectra of Brilliant Blue stain were recorded at different time intervals between 450 and 850 nm wavelengths. There was a frequent decrease in the absorbance peak which clearly indicates the Brilliant Blue degradation due to the decomposition process. Degradation was calculated using the formula Degradation formula (%) = $(\text{Ext}_0 - \text{Ext})/\text{Ext}_0 \times 100$, where Ext_0 is initial and Ext final concentration of Brilliant Blue dye. WO_3 nanoparticles alone degraded around 60% of brilliant blue in 40 min, whereas 90% of degradation was observed in 40 min when $\text{WO}_3\text{-ZnO}$ nanocomposite was administered. The slope of the plot in $(\text{Ext}_t/\text{Ext}_0)$ versus reaction time was apparently found to be first-order reaction and its kinetics in both the cases. The slope of this plot gives

a value of the rate constant (k) and is found to be $k = 7.01 \times 10^{-3} \text{ s}^{-1}$ for $\text{WO}_3\text{-ZnO}$ nanocomposite and $0.346 \text{ cm}^{-3} \text{ s}^{-1}$ for WO_3 nanoparticles [17].

Jun Wang et al. in the sonocatalytic degradation process of acid red B and Rhodamine B dye, ZnO powder was used as such by heating it at $300 \text{ }^\circ\text{C}$ for 2 h. The activated ZnO powder was mixed with acid red B and Rhodamine B solutions, respectively. After a proper stirring to make a good dispersion, was placed in an ultrasound apparatus and irradiated. The UV-vis spectra of acid red B and Rhodamine B solutions during degradation were determined at regular intervals. The experimental conditions were initial concentration of 10 mg/L ZnO nano powder, TiO_2 addition amount of 1.0 mg/L , initial acidity of $\text{pH } 7.0$, systemic temperature of $25.0 \pm 0.2 \text{ }^\circ\text{C}$, ultrasonic irradiation time of 60 min and total volume of 50 mL were collected to analyse the sonocatalytic activity of nanosized ZnO powder. It was found that the characteristic absorption peaks of both Acid Red B and Rhodamine B solutions at 510 nm and 560 nm, respectively, declined under ultrasonic irradiation in the presence of nanosized ZnO powder. The peaks declined as a result of decomposition and showed great results when compared to other samples with onefold ultrasonic degradation and onefold adsorption of the nanosized ZnO powder. In comparison with Acid Red B and Rhodamine B, the enhancement effect of nanosized ZnO powder on the sonocatalytic degradation of Acid Red B was much better than that of Rhodamine B. Degradation ratio of Acid Red B in the presence of nanosized ZnO powder was 71.2% in 60 min ultrasonic irradiation, while it was only 39.1% for Rhodamine B at the same time. In the absence of ultrasound irradiation, the degradation percentage of Acid Red B and Rhodamine B was 22.3% and 8.2%, respectively. Here also the reaction kinetics was inferred as first-order reaction. The rate constant for Acid Red B is much greater than that for Rhodamine B, which is 0.016 min^{-1} and 0.0066 min^{-1} , respectively, and both confirmed pseudo first-order kinetic reactions. As initial concentration of dye waste water increases, the degradation ratio gradually decreases because of the increase in dye molecules on the surface of ZnO particles. This will hinder OH^- ions from being absorbed by ZnO nanoparticles; thus lowering the formation rate of hydroxyl radicals (OH^-), and consequently, it affects negatively the degradation efficiency. Degradation ratios of both Acid Red B and Rhodamine B increased with the increase of nanosized ZnO powder up to 1.0 g/L after which Rhodamine showed a slight decrease in the degradation ratio which may be due to the nearness and aggregation of nanosized ZnO particles [52] (Fig. 1).

5 Effects of Parameters on ZnO Dye Degradation

5.1 Effect of pH on the Photocatalytic Activity

The effect of pH on the adsorption efficiency of the materials used for adsorption and the removal capacity of the adsorbate or adsorbent was evaluated [39]. The

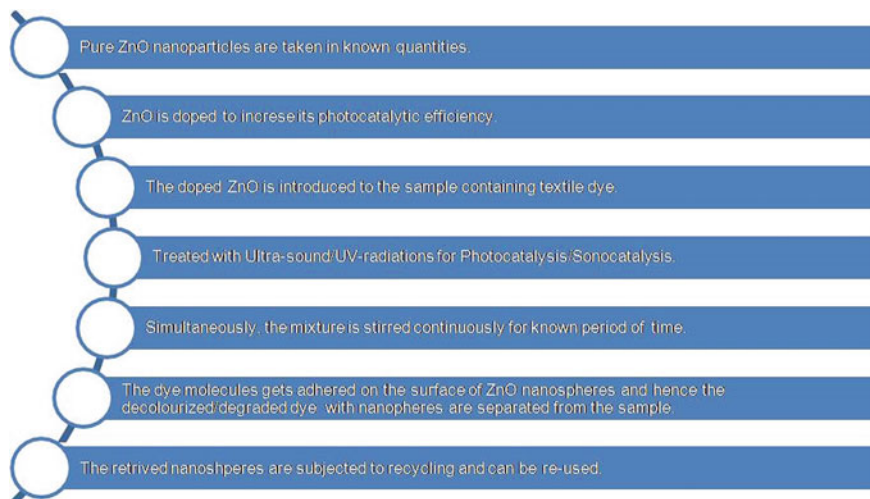


Fig. 1 Schematic representation of process of degradation

studies where the influence of pH was considered as criteria that can alter the photocatalytic process were conducted in the pH range of 4–10 using ZnO nanosphere catalysts dissolved in dye solution in an ideal reaction time. The adjustments of pH in the solution were maintained using acidic and basic solutions like HCl and NaOH, respectively. The rate of degradation and bleaching of dye are influenced or affected by the change in pH. The rate of degradation and bleaching of dye were observed to be high or efficient at pH 6 which is a bit acidic. The graphical elucidation resulted due to the variation of pH has shown that the efficiency of photodegradation was maintained high and raised till pH 6. After a slight constant curve, the graph declined when there is an increase in the pH number (that is, >pH 6 viz. 7–14). In the above study, the effect of pH in dye degradation is dependent on semiconductor oxide (CuO, WO₃, NiO etc.) that causes acid–base equilibrium which regulates the surface dynamics of nanocatalyst activities [47, 54]. Hence, the experiments use pH 6 as an optimum pH to carry out photocatalytic dye degradation. The effect of pH in the removal or adsorption efficiency (surface chemistry of nanocatalysts) is due to the variation of electrostatic force of attraction on ZnO nanospheres where the dye molecules adhere. Due to the variation of pH in the medium, the increase in the pH to optimum levels (i.e., pH 6) attracts the dye molecules and decrease in the optimum pH or any pH which is more than pH 6 causes the removal of dye and in turn decreases the activity of nanoparticles as the electrostatic force of attraction is directly proportional to the adsorption and removal of dye molecules on the surface of nanoparticles [57]. At the basic pH, that is, pH 9, the surface of ZnO nanoparticle possesses positive charges [8]. Hence, due to the property of electrostatic force of attraction, any pollutant that carries a negative charge (anion pollutant) moves to the adsorbent surface of nanoparticles [45]. The pK_a value of dye with elevated pH of the solution, the dye exists with negative ion for and gets adhered to the adsorbent surface

of nanoparticles. Thus, the increase in the pH to 6, the rate of adsorption of anionic pollutant or dye and the degradation efficiency of ZnO nanoparticles increases. At ideal pH 6, the rate of dye degradation and bleaching rate increases. The above property can be accredited to the decreased oxidation potential of OH^- radical that has an impact on pH as hydroxyl radical contributes to increasing the pH of the solution [29]. Simultaneously, the increased hydroxyl ions also affect the surface adhering activity of ZnO nanoparticles by inhibiting the binding of dye molecules that are anionic in nature to the surface of photocatalyst [41].

5.2 Effect of ZnO Nanospheres Dose

To observe the effect of ZnO nanospheres or photocatalysts concentration on the rate of degradation and decolouration of dye molecules, a variable range of photocatalyst nanospheres were introduced to the solution for a certain period of time at the optimum pH 6 with certain initial dye concentration where the range of concentration of nanosphere lies in between 50 and 300 mg/L. The findings and reports proved that the rate of degradation and rate of decolourization were elevated due to the increase in the concentration of photocatalytic nanospheres to a higher range compared to initial concentration. In further increase in the concentration of catalyst, there is no raise in the degradation and decolourization of dye with the increase in concentration of catalyst. When the concentration was further more enhanced, the decrease in the photocatalyst activity causes less decolourization and degradation of dye. Henceforth, this shows there exists an optimum concentration of photocatalyst for its enhanced or ideal activity. Until a certain concentration, the decolourization and degradation is directly proportional to the activity of photocatalytic nanospheres. The increased release of hydroxyl radicals are due to the catalytic activity of nanospheres crumbles the rate of degradation and decolourization. When the concentration of nanoparticles is increased, the solution turns turbid, a milky white turbidity can be observed which prevents the penetration of UV light that causes decreased effect of UV irradiation. This phenomenon causes decreased efficiency in dye degradation. Thus, the concentration of nanosphere where it shows the ideal activity in decolourizing and degrading the dye becomes a critical criterion to be considered for further investigation. The ideal concentration of ZnO nanospheres is determined to be 100 mg/L with the corresponding and correlating factors that are known [14, 55].

5.3 Effect of Calcination (Elevated Temperature) on the Optical Activity of ZnO Nanospheres

Range of temperatures $^{\circ}\text{C}$ was used to determine the effect of calcination on the photocatalytic activity of ZnO nanospheres. The effects of calcinated photocatalyst

are increased with the elevation of temperatures in the process of dye decolourization and degradation. The photocatalytic activity is elevated with the increase until a certain temperature and then the activity becomes constant producing a plateau-like curve when plotted. The above phenomenon is attributed to the carbon substrate residue CTAB adhered on the surface of nanoparticles which affects the photocatalytic activity. The highest possible or efficient or ideal calcination temperature of 450 °C is preferred by the conducted experiments where the complete burning of CTAB happens [42].

5.4 Influence of Stirring

To study the effect of stirring on the rate of decolourization and dye degradation was studied under the above-mentioned ideal conditions (where the time 50 min, ideal pH 6, initial dye concentration of 10 mg/mL and the concentration of ZnO nanospheres 100 mg/L). The stirring results in the elevated rate of dye degradation and decolourization. Thus, the effect of rate of stirring is directly proportional to the increased dye photocatalytic activity. The stirring causes the release of trapped oxygen in between the nanosphere and removes hydroxyl radicals that are present, thus increasing in surface area for the adsorption of dye. To note, the stirring of the solution causes a decrease in the rate of equilibrium period hence increasing the rate of diffusion of dye molecules that adhere to the surface of photocatalysts [4].

5.5 Effect of Oxygen Concentration

The effect of concentration of oxygen in the photocatalyst has an impact on the rate of dye degradation and decolourization. A current of air containing oxygen and nitrogen was conducted through the solution to analyse the efficiency of ZnO photocatalyst. The procedure was conducted under the ideal condition (where the time 50 min, ideal pH 6, initial dye concentration of 10 mg/mL and the concentration of ZnO nanospheres 100 mg/L) and the gas containing nitrogen was passed through the solution for 2.5 min. The passage of nitrogen caused the removal of oxygen that decreased the activity of photocatalyst. Thus, it is determined that the presence of oxygen in the solution causes increased efficiency of photocatalyst nanospheres in dye degradation and decolourization. The free oxygen radicals carrying negative charge attributes to the oxidation of hydroxyl radicals resulting in the formation of hydrogen peroxide (H₂O₂) and molecular oxygen (O₂). Thus increases the efficiency of the photocatalytic ZnO nanospheres [28].

5.6 Recycling of the Photocatalytic ZnO Nanospheres

The recycling of photocatalytic ZnO nanospheres has its importance in the economic point of view. The reused photocatalytic ZnO nanospheres can be used by recovering them from the sources where the decolourization and degradation were already being conducted and can be utilized for further photocatalytic activities. To reuse the pre-used ZnO nanospheres the efficiency should be retrieved. The recovery of pure ZnO nanospheres by removal of the decolourized and degraded dye and impurities are done by subjecting them into multiple cycles of centrifugation under >4000 rpm. Thus, the impurities and degraded dyes are removed also by rinsing the centrifuged ZnO nanospheres using ethanol and bi-distilled water. The duly recovered and purified ZnO nanospheres can be reused in dye degradation. The efficiency or the capacity of ZnO nanoparticles that are recovered by recycling are comparatively lower than that of the freshly prepared or unused ZnO nanospheres. The recycled nanospheres also show a decrease in its activity of rate of decolourization and degradation processes in multiple usage [42] (Fig. 2).



Fig. 2 Schematic representation of properties attributed to ZnO nanospheres

6 Discussions

Since ages, textile industries have been using a lot of variant dyes that are washed out as waste through outlets to the natural water bodies. The content of these outlets might be organic, inorganic, natural or synthetic but are hazardous to the biome present in the water bodies. Despite being hazardous they are also non-biodegradable. Different ways of approaches have been conducted till date to degrade the dyes, among which the use of nanospheres or nanoparticles are photocatalysts or sonocatalysts that are known to successfully decolourize or bleach and degrade the dyes. Few transition metal oxides are well known for their property of adsorption due to their capacity to produce lone-pair of electrons and holes by providing the dyes to adhere on its surface. Different transition metals like TiO_2 , WO_3 , Fe_2O_3 , ZnO , MgO and other transition metal oxides are used for the preparation of photocatalytic nanospheres among which ZnO is known to be stable, efficient, affordable and environment-friendly catalyst. ZnO is a semiconductor metal oxide which has the capacity to hydrolyze aqueous solutions. When ZnO nanospheres are used to decolourize and degrade the dye pollutants present in the water under the influence of UV irradiation causes hydrolysis of water producing OH^- and H^+ . These OH^- and H^+ might mask the ability of ZnO to act as photocatalyst by acting as electron scavengers.

To avoid this phenomenon of electron scavenging by OH^- and H^+ species, ZnO nanocatalysts are doped. Doping helps in the generation of charge carriers for the degradation of dye pollutants by recombining photogenerated electron-hole pair. Thus, it helps to achieve high photocatalytic efficiency.

There are different studies that are carried out to dope ZnO with other narrow band gap semiconductors. This process is known as Co-doping as it attributes more qualities of photocatalysis when combined with ZnO nanospheres when compared to pure ZnO nanospheres. There are different ways of approach in dye degradation due to the multiple catalytic properties of ZnO or doped ZnO , they are photocatalysis, sonocatalysis under the influence of UV irradiation, IR radiation, natural light treatment, hydrothermal activity, combustion and calcination at high temperature.

The applications of nanoparticles are seen in diverse areas such as agriculture, animal husbandry, chemical sciences, medical sciences, biotechnology, electronic engineering veterinary science etc. They have been also used in medicinal treatments, fabrication of devices like solar cells, oxide fuel batteries for energy storage, as biosensors, cosmetic products, UV protection fabrics and so on. Antibacterial agents such as antiseptics, antidandruff shampoos, baby powder etc. contain ZnO particles. The antibacterial property and other biological functioning of ZnO nanoparticles depend on the concentration, morphology, size, healing, temperature and affinity between the bacterial cells and ZnO . On the other hand, Ag/NPs showed an effective antibacterial, antifungal and antiviral property.

Semiconductor-assisted photocatalytic degradation is found to be an effective method to degrade organic compounds present in the portable water sources. Apart from physiochemical methods like adsorption, nanofiltration and electrochemical methods, Advanced Oxidative Process (AOPs) is proved to be a good technique for

the degradation of organic pollutants. Sonocatalysis is another emerging AOP to remove persistent organic compounds.

Sonocatalysts are active under ultrasonic irradiation and have a high rate of degradation of organic contaminants. TiO_2 , ZnO , Cu_2S , CdS , ZnS , ZnO-NRs-AC and Cu:ZnS-NPs-AC , $\text{MIL-101(Cr)/RGO/ZnFe}_2\text{O}_4$ and $\text{CoFe}_2\text{O}_4@\text{ZnS}$ are various catalysts that show good sonocatalytic activities. WO_3 is one of the promising photocatalysts for many opto-electronic applications etc. WO_3/ZnO nanorods synthesized via Hydrothermal-deposition technique are found to be highly effective in the degradation of 2,4-dichlorophenoxy acetic acid (2,4-D) under natural sunlight. At 600 °C calcination temperature WO_3/ZnO composites with 2 wt% concentration of WO_3 showed doubled photocatalytic activity as compared to pure ZnO . TiO_2 (3.37 eV) and ZnO (3.18 eV) are wide band gap semiconductor metal oxides, which have great importance due to their high catalytic efficiency. Noble metals like Ag/Pt can act as electron sinks thereby reducing the electron-hole recombination and charge separation. Noble metal/ ZnO has the capacity to enhance the corrosion resistance, to improve the photocatalytic efficiency and photostability. Ag ions have attracted attention for their combined property of both photoactivity and antibacterial properties. Solvothermal method is another technique of preparing large-scale ZnO nanostructures. Cetyltrimethylammonium bromide (CTAB) has been used in this solvothermal technique as organic dispersant. They interact with ZnO to form nanowires on the surface of ZnO by the synergic effect of the surfactant and the solvent (ethanol). Solvothermal method helps in the deposition of noble-NPs on the ZnO-NWs and thereby obtains nanoparticles with a high surface to volume ratio, even distribution of noble metal etc. Flame aerosol synthesis is an alternate method used to prepare nanoscale materials commercially at a low cost. Flame Spray Pyrolysis (FSP) is used in particular for one-step drying synthesis of high surface area noble metal-laden catalysis. This method provides highly pure particles, control of particle size and good crystalline structure on one step.

Aquatic system is contaminated due to the growth of industrialization which releases chemicals like organic dyes, gases, oils, heavy metals which are hazardous to plants and animals. According to WHO, contaminated water caused many diseases like Giardiasis, Cholera, Viral gastroenteritis etc. which kills millions of people each year. The dye from textile industries, tanneries, kraft mills and other industrial wastes are non-biodegradable chemicals and contribute to the elevated levels of Biological Oxygen Demand (BOD), Chemical Oxygen Demand (COD), pH and colour. Hence there is a requirement for an efficient, harmless and environment-friendly technique to degrade the pollutants. Nanoparticles of size ranging from 1 to 100 nm have been studied in a wide range for their remarkable properties like catalytic degradation, antibacterial agents etc. Various studies have been conducted regarding the use of ZnO nanospheres as dye degrading components. Few among them are tabulated (Table 1).

Table 1 Various studies on dye degradation using different combinations of ZnO nanocomposites

Sl. no	Dye degraded	Nanocomposites used	Mode of degradation	Photo-spectrum	Type of degradation	References
1	Methylene blue	CuO/ZnO	Thermal decomposition	Visible light spectrum	Photocatalytic	[27]
2	Methylene blue	CuO	Carbothermal	Sunlight irradiation	Photocatalytic	[27]
3	Methylene blue	WO ₃	Precipitation grinding method	Sunlight	Photocatalytic	[1, 17, 56]
4	Methylene blue	N/ZnO	Hydrothermal decomposition	UV-Visible light range	Photocatalytic	[20, 24]
5	Methylene blue	N/ZnO	Combustion reaction	Visible light	Photocatalytic	[37, 46]
6	Methylene blue	Ni/ZnO	Co-gel/Co-precipitation techniques	UV-Visible spectrum	Photocatalytic	[11, 27]
7	Methylene blue and eosin Y	ZnO		UV irradiation (16 W lamp as source)	Photocatalytic	[7]
8	Methyl orange	CuO/ZnO	Thermal decomposition	Visible light spectrum	Photocatalytic	[27]
9	Methyl orange	CuO	Xe-Lamp	Photo-degradation	Photocatalytic	[27]
10	Azo Rhodamine b	CuO	Xe-Lamp	Photo-degradation	Photocatalytic	[27]
11	Brilliant blue	WO ₃ -ZnO	-	Ultrasonic irradiation	Sonocatalytic	[17]
12	Methylene blue	ZnO-green synthesized Ag	-	Sunlight	Photocatalytic	[19]
13	Methylene blue	ZnO, ZnO/Ag, ZnO/Pt	Mercury vapour lamp	UV light irradiation	Photocatalytic	[32]
14	Methylene blue	ZnO, Au/ZnO, Pt/ZnO	UV light 2 _ 15 W UV tube	UV irradiation	Photocatalytic	[36]
15	Methylene blue	Ag/ZnO	-	Visible irradiations	Photocatalytic	[34]
16	Acid red B and Rhodamine B	ZnO	-	Ultrasonic irradiation	Sonocatalytic	[52]
17	Coomassie brilliant blue R-250 dye	Green synthesized ZnO	-	Sunlight	Photocatalytic	[44]

7 Conclusion

Due to the release of toxic dyes from textile industry into the natural water bodies, there are many hazardous conditions being formed that spoils the biome and upsets the ecosystem [7, 47]. To solve this, various approaches are being done among which ZnO dye degradation is one of the reliable and efficient methods [11, 42]. To conclude with the above work, reviewing different experiments and comparison of dye degradation using ZnO as a basic semiconductor metal ion nanoparticle reflects that the use of ZnO is more appropriate because of its attributing properties being efficient and environment-friendly. As stability place an important role in any chemical reactions concerned with approaches of environmental application that helps in the betterment of conditions like pollution, wastewater treatment etc. ZnO (pure or doped form) [23, 35, 37] has excellent properties of remaining unaffected and also contributing to degradation. Natural solar radiations and ultraviolet radiations can be used to enhance the properties of ZnO in dye degradation. The usage of ultrasound to create higher efficiency of the nanoparticles results in sonocatalysis. These properties have positive contribution to the field of environmental application, ZnO nanoparticles are highly credited among other semiconductor nanoparticles.

Bibliography

1. Adhikari S, Sarkar D, Madras G (2015) Highly efficient $\text{WO}_3\text{-ZnO}$ mixed oxides for photocatalysis. *RSC Adv* 5(16):11895–11904. <https://doi.org/10.1039/c4ra13210f>
2. Anandan S, Wu JJ (2014) Ultrasound assisted synthesis of $\text{TiO}_2\text{-WO}_3$ heterostructures for the catalytic degradation of Tergitol (NP-9) in water. *Ultrason Sonochem* 21(4):1284–1288. <https://doi.org/10.1016/j.ultsonch.2014.01.014>
3. Anju SG, Yesodharan S, Yesodharan EP (2012) Zinc oxide mediated sonophotocatalytic degradation of phenol in water. *Chem Eng J* 189–190:84–93. <https://doi.org/10.1016/j.cej.2012.02.032>
4. Bagheri AR, Ghaedi M, Asfaram A, Jannesar R, Goudarzi A (2017) Design and construction of nanoscale material for ultrasonic assisted adsorption of dyes: application of derivative spectrophotometry and experimental design methodology. *Ultrason Sonochem* 35:112–123. <https://doi.org/10.1016/j.ultsonch.2016.09.008>
5. Bustos-Torres KA, Vazquez-Rodriguez S, la Cruz AM de, Sepulveda-Guzman S, Benavides R, Lopez-Gonzalez R, Torres-Martínez LM (2017) Influence of the morphology of ZnO nano-materials on photooxidation of polypropylene/ZnO composites. *Mater Sci Semicond Process* 68(May):217–225. <https://doi.org/10.1016/j.mssp.2017.06.023>
6. Carraway ER, Hoffman AJ, Hoffmann MR (1994) Photocatalytic oxidation of organic acids on quantum-sized semiconductor colloids. *Environ Sci Technol* 28(5):786–793. <https://doi.org/10.1021/es00054a007>
7. Chakrabarti S, Dutta BK (2004) Photocatalytic degradation of model textile dyes in wastewater using ZnO as semiconductor catalyst. *J Hazard Mater* 112(3):269–278. <https://doi.org/10.1016/j.jhazmat.2004.05.013>
8. Daneshvar N, Aber S, Seyed Dorraji MS, Khataee AR, Rasoulifard MH (2007) Photocatalytic degradation of the insecticide diazinon in the presence of prepared nanocrystalline ZnO powders under irradiation of UV-C light. *Sep Purif Technol* 58(1):91–98. <https://doi.org/10.1016/j.seppur.2007.07.016>

9. Dzsaber S, Negyedi M, Bernáth B, Gyüre B, Fehér T, Kramberger C, Pichler T, Simon F (2015) A Fourier transform Raman spectrometer with visible laser excitation. *J Raman Spectrosc* 46(3):327–332. <https://doi.org/10.1002/jrs.4641>
10. Ebrahimi R, Maleki A, Zandsalimi Y, Ghanbari R, Shahmoradi B, Rezaee R, Safari M, Joo SW, Daraei H, Harikaranahalli Puttaiah S, Giahi O (2019) Photocatalytic degradation of organic dyes using WO₃-doped ZnO nanoparticles fixed on a glass surface in aqueous solution. *J Ind Eng Chem* 73:297–305. <https://doi.org/10.1016/j.jiec.2019.01.041>
11. Hameed A, Montini T, Gombac V, Fornasiero P (2009) Photocatalytic decolourization of dyes on NiO–ZnO nano-composites. *Photochem Photobiol Sci* 8(5):677–682. <https://doi.org/10.1039/b817396f>
12. Havrdova M, Polakova K, Skopalik J, Vujtek M, Mokdad A, Homolkova M, Tucek J, Nebesarova J, Zboril R (2014) Field emission scanning electron microscopy (FE-SEM) as an approach for nanoparticle detection inside cells. *Micron* 67:149–154. <https://doi.org/10.1016/j.micron.2014.08.001>
13. Hollerith C, Wernicke D, Bühler M, Feilitzsch FV, Huber M, Höhne J, Hertrich T, Jochum J, Phelan K, Stark M, Simmnacher B, Weiland W, Westphal W (2004) Energy dispersive X-ray spectroscopy with microcalorimeters. *Nucl Instrum Methods Phys Res Sect A* 520(1–3):606–609. <https://doi.org/10.1016/j.nima.2003.11.327>
14. Hossaini H, Moussavi G, Farrokhi M (2017) Oxidation of diazinon in cns-ZnO/LED photocatalytic process: catalyst preparation, photocatalytic examination, and toxicity bioassay of oxidation by-products. *Sep Purif Technol* 174:320–330. <https://doi.org/10.1016/j.seppur.2016.11.005>
15. Huang Z, Maness PC, Blake DM, Wolfrom EJ, Smolinski SL, Jacoby WA (2000) Bactericidal mode of titanium dioxide photocatalysis. *J Photochem Photobiol A* 130(2–3):163–170. [https://doi.org/10.1016/S1010-6030\(99\)00205-1](https://doi.org/10.1016/S1010-6030(99)00205-1)
16. Hunge YM, Mahadik MA, Moholkar AV, Bhosale CH (2017) Photoelectrocatalytic degradation of oxalic acid using WO₃ and stratified WO₃/TiO₂ photocatalysts under sunlight illumination. *Ultrason Sonochem* 35:233–242. <https://doi.org/10.1016/j.ultsonch.2016.09.024>
17. Hunge YM, Yadav AA, Mathe VL (2018) Ultrasound assisted synthesis of WO₃–ZnO nanocomposites for brilliant blue dye degradation. *Ultrason Sonochem* 45(January):116–122. <https://doi.org/10.1016/j.ultsonch.2018.02.052>
18. Hunge YM, Yadav AA, Mohite BM, Mathe VL, Bhosale CH (2018) Photoelectrocatalytic degradation of sugarcane factory wastewater using WO₃/ZnO thin films. *J Mater Sci Mater Electron* 29(5):3808–3816. <https://doi.org/10.1007/s10854-017-8316-1>
19. Jadhav P, Shinde S, Suryawanshi SS, Teli SB, Patil PS, Ramteke AA, Hiremath NG, Prasad NR (2020) Green AgNPs decorated ZnO nanocomposites for dye degradation and antimicrobial applications. *Eng Sci* 12:79–94. <https://doi.org/10.30919/es8d1138>
20. Kabir R, Saifullah MAK, Ahmed AZ, Masum SM, Molla MAI (2020) Synthesis of n-doped zno nanocomposites for sunlight photocatalytic degradation of textile dye pollutants. *J Compos Sci* 4(2). <https://doi.org/10.3390/jcs4020049>
21. Kanade KG, Kale BB, Baeg JO, Lee SM, Lee CW, Moon SJ, Chang H (2007) Self-assembled aligned Cu doped ZnO nanoparticles for photocatalytic hydrogen production under visible light irradiation. *Mater Chem Phys* 102(1):98–104. <https://doi.org/10.1016/j.matchemphys.2006.11.012>
22. Kavitha MK, Pillai SC, Gopinath P, John H (2015) Hydrothermal synthesis of ZnO decorated reduced graphene oxide: understanding the mechanism of photocatalysis. *J Environ Chem Eng* 3(2):1194–1199. <https://doi.org/10.1016/j.jece.2015.04.013>
23. Khalid NR, Hammad A, Tahir MB, Rafique M, Iqbal T, Nabi G, Hussain MK (2019) Enhanced photocatalytic activity of Al and Fe co-doped ZnO nanorods for methylene blue degradation. *Ceram Int* 45(17):21430–21435. <https://doi.org/10.1016/j.ceramint.2019.07.132>
24. Khataee A, Karimi A, Arefi-Oskoui S, Darvishi Cheshmeh Soltani R, Hanifehpour Y, Soltani B, Joo SW (2015) Sonochemical synthesis of Pr-doped ZnO nanoparticles for sonocatalytic degradation of acid red 17. *Ultrason Sonochem* 22:371–381. <https://doi.org/10.1016/j.ultsonch.2014.05.023>

25. Kuriakose S, Avasthi DK, Mohapatra S (2015) Effects of swift heavy ion irradiation on structural, optical and photocatalytic properties of ZnO–CuO nanocomposites prepared by carbothermal evaporation method. *Beilstein J Nanotechnol* 6(1):928–937. <https://doi.org/10.3762/bjnano.6.96>
26. Lam SM, Sin JC, Abdullah AZ, Mohamed AR (2013) Investigation on visible-light photocatalytic degradation of 2,4-dichlorophenoxyacetic acid in the presence of MoO₃/ZnO nanorod composites. *J Mol Catal A Chem* 370:123–131. <https://doi.org/10.1016/j.molcata.2013.01.005>
27. Li B, Wang Y (2010) Facile synthesis and photocatalytic activity of ZnO–CuO nanocomposite. *Superlattices Microstruct* 47(5):615–623. <https://doi.org/10.1016/j.spmi.2010.02.005>
28. Litter MI (2005) Introduction to photochemical advanced oxidation processes for water treatment. In: *Environmental photochemistry part II*, vol 2, Issue September, pp 325–366. <https://doi.org/10.1007/b138188>
29. Lucas MS, Peres JA (2006) Decolorization of the azo dye reactive black 5 by Fenton and photo-Fenton oxidation. *Dyes Pigm* 71(3):236–244. <https://doi.org/10.1016/j.dyepig.2005.07.007>
30. Ma H, Cheng X, Ma C, Dong X, Zhang X, Xue M, Zhang X, Fu Y (2013) Synthesis, characterization, and photocatalytic activity of N-doped ZnO/ZnS composites. *Int J Photoenergy* 2013. <https://doi.org/10.1155/2013/625024>
31. Moroni M, Borrini D, Calamai L, Dei L (2005) Ceramic nanomaterials from aqueous and 1,2-ethanediol supersaturated solutions at high temperature. *J Colloid Interface Sci* 286(2):543–550. <https://doi.org/10.1016/j.jcis.2005.01.097>
32. Muñoz-Fernandez L, Sierra-Fernandez A, Milošević O, Rabanal ME (2016) Solvothermal synthesis of Ag/ZnO and Pt/ZnO nanocomposites and comparison of their photocatalytic behaviors on dyes degradation. *Adv Powder Technol* 27(3):983–993. <https://doi.org/10.1016/j.apt.2016.03.021>
33. Pal B, Sharon M (2002) Enhanced photocatalytic activity of highly porous ZnO thin films prepared by sol-gel process. *Mater Chem Phys* 76(1):82–87. [https://doi.org/10.1016/S0254-0584\(01\)00514-4](https://doi.org/10.1016/S0254-0584(01)00514-4)
34. Panchal P, Paul DR, Sharma A, Choudhary P, Meena P, Nehra SP (2020) Biogenic mediated Ag/ZnO nanocomposites for photocatalytic and antibacterial activities towards disinfection of water. *J Colloid Interface Sci* 563:370–380. <https://doi.org/10.1016/j.jcis.2019.12.079>
35. Pascariu P, Tudose IV, Sucheia M, Koudoumas E, Fifere N, Airinei A (2018) Preparation and characterization of Ni, Co doped ZnO nanoparticles for photocatalytic applications. *Appl Surf Sci* 448:481–488. <https://doi.org/10.1016/j.apsusc.2018.04.124>
36. Pawinrat P, Mekasuwandumrong O, Panpranot J (2009) Synthesis of Au-ZnO and Pt-ZnO nanocomposites by one-step flame spray pyrolysis and its application for photocatalytic degradation of dyes. *Catal Commun* 10(10):1380–1385. <https://doi.org/10.1016/j.catcom.2009.03.002>
37. Prabakaran E, Pillay K (2019) Synthesis of N-doped ZnO nanoparticles with cabbage morphology as a catalyst for the efficient photocatalytic degradation of methylene blue under UV and visible light. *RSC Adv* 9(13):7509–7535. <https://doi.org/10.1039/C8RA09962F>
38. Prencipe I, Dellasega D, Zani A, Rizzo D, Passoni M (2015) Energy dispersive X-ray spectroscopy for nanostructured thin film density evaluation. *Sci Technol Adv Mater* 16(2). <https://doi.org/10.1088/1468-6996/16/2/025007>
39. Rahmani M, Kaykhaii M, Sasani M (2018) Application of Taguchi L16 design method for comparative study of ability of 3A zeolite in removal of Rhodamine B and Malachite green from environmental water samples. *Spectrochim Acta Part A Mol Biomol Spectrosc* 188:164–169. <https://doi.org/10.1016/j.saa.2017.06.070>
40. Reddy IN, Reddy CV, Shim J, Akkinapally B, Cho M, Yoo K, Kim D (2020) Excellent visible-light driven photocatalyst of (Al, Ni) co-doped ZnO structures for organic dye degradation. *Catal Today* 340:277–285. <https://doi.org/10.1016/j.cattod.2018.07.030>
41. Saini J, Garg VK, Gupta RK, Kataria N (2017) Removal of Orange G and Rhodamine B dyes from aqueous system using hydrothermally synthesized zinc oxide loaded activated carbon (ZnO-AC). *J Environ Chem Eng* 5(1):884–892. <https://doi.org/10.1016/j.jece.2017.01.012>

42. Saleh SM (2019) ZnO nanospheres based simple hydrothermal route for photocatalytic degradation of azo dye. *Spectrochim Acta Part A Mol Biomol Spectrosc* 211:141–147. <https://doi.org/10.1016/j.saa.2018.11.065>
43. Sing KSW (1989) The use of gas adsorption for the characterization of porous solids. *Colloids Surf* 38(1):113–124. [https://doi.org/10.1016/0166-6622\(89\)80148-9](https://doi.org/10.1016/0166-6622(89)80148-9)
44. Singh K, Singh J, Rawat M (2019) Green synthesis of zinc oxide nanoparticles using Punica Granatum leaf extract and its application towards photocatalytic degradation of Coomassie brilliant blue R-250 dye. *SN Appl Sci* 1(6). <https://doi.org/10.1007/s42452-019-0610-5>
45. Štastná M, Trávníček M, Šlais K (2005) New azo dyes as colored isoelectric point markers for isoelectric focusing in acidic pH region. *Electrophoresis* 26(1):53–59. <https://doi.org/10.1002/elps.200406088>
46. Sudrajat H, Babel S (2017) A novel visible light active N-doped ZnO for photocatalytic degradation of dyes. *J Water Process Eng* 16:309–318. <https://doi.org/10.1016/j.jwpe.2016.11.006>
47. Tanaka K, Padermpole K, Hisanaga T (2000) Photocatalytic degradation of commercial azo dyes. *Water Res* 34(1):327–333. [https://doi.org/10.1016/S0043-1354\(99\)00093-7](https://doi.org/10.1016/S0043-1354(99)00093-7)
48. Tang WZ, An H (1995) UV/TiO₂ photocatalytic oxidation of commercial dyes in aqueous solutions. *Chemosphere* 31(9):4157–4170. [https://doi.org/10.1016/0045-6535\(95\)80015-D](https://doi.org/10.1016/0045-6535(95)80015-D)
49. Turan R, Perovic DD, Houghton DC (1996) Mapping electrically active dopant profiles by field-emission scanning electron microscopy. *Appl Phys Lett* 69(11):1593–1595. <https://doi.org/10.1063/1.117041>
50. Ullah R, Dutta J (2008) Photocatalytic degradation of organic dyes with manganese-doped ZnO nanoparticles. *J Hazard Mater* 156(1–3):194–200. <https://doi.org/10.1016/j.jhazmat.2007.12.033>
51. Velavan S, Amargeetha A (2018) X-ray diffraction (XRD) and energy dispersive spectroscopy (EDS) analysis of silver nanoparticles synthesized from erythrina indica flowers. *Nanosci Technol Open Access* 5(1):1–5. <https://doi.org/10.15226/2374-8141/5/1/00152>
52. Wang J, Jiang Z, Zhang Z, Xie Y, Wang X, Xing Z, Xu R, Zhang X (2008) Sonocatalytic degradation of acid red B and Rhodamine B catalyzed by nano-sized ZnO powder under ultrasonic irradiation. *Ultrason Sonochem* 15(5):768–774. <https://doi.org/10.1016/j.ultsonch.2008.02.002>
53. Xie J, Zhou Z, Lian Y, Hao Y, Liu X, Li M, Wei Y (2014) Simple preparation of WO₃-ZnO composites with UV-Vis photocatalytic activity and energy storage ability. *Ceram Int* 40(8 Part A):12519–12524. <https://doi.org/10.1016/j.ceramint.2014.04.106>
54. Yang TCK, Wang SF, Tsai SHY, Lin SY (2001) Intrinsic photocatalytic oxidation of the dye adsorbed on TiO₂ photocatalysts by diffuse reflectance infrared Fourier transform spectroscopy. *Appl Catal B* 30(3–4):293–301. [https://doi.org/10.1016/S0926-3373\(00\)00241-1](https://doi.org/10.1016/S0926-3373(00)00241-1)
55. Youssef Z, Colombeau L, Yesmurzayeva N, Baros F, Vanderesse R, Hamieh T, Toufaily J, Frochot C, Roques-Carmes T (2018) Dye-sensitized nanoparticles for heterogeneous photocatalysis: cases studies with TiO₂, ZnO, fullerene and graphene for water purification. *Dyes Pigments* (Elsevier Ltd.) 159:49–71. <https://doi.org/10.1016/j.dyepig.2018.06.002>
56. Yu C, Yang K, Shu Q, Yu JC, Cao F, Li X (2011) Preparation of WO₃/ZnO composite photocatalyst and its photocatalytic performance. *Cuihua Xuebao/Chin J Catal* 32(4):555–565. [https://doi.org/10.1016/s1872-2067\(10\)60212-4](https://doi.org/10.1016/s1872-2067(10)60212-4)
57. Zbair M, Anfar Z, Ait Ahsaine H, El Alem N, Ezahri M (2018) Acridine orange adsorption by zinc oxide/almond shell activated carbon composite: operational factors, mechanism and performance optimization using central composite design and surface modeling. *J Environ Manag* 206:383–397. <https://doi.org/10.1016/j.jenvman.2017.10.058>
58. Zhang L, Qi H, Yan Z, Gu Y, Sun W, Zewde AA (2017) Sonophotocatalytic inactivation of E. coli using ZnO nanofluids and its mechanism. *Ultrason Sonochem* 34:232–238. <https://doi.org/10.1016/j.ultsonch.2016.05.045>